

Topology optimization of metal nanostructures for localized surface plasmon resonances

Yongbo Deng¹ · Zhenyu Liu² · Chao Song¹ · Peng Hao¹ · Yihui Wu¹ · Yongmin Liu^{3,4} · Jan G. Korvink⁵

Received: 31 July 2014 / Revised: 28 December 2014 / Accepted: 6 March 2015 / Published online: 24 December 2015
© Springer-Verlag Berlin Heidelberg 2015

Abstract This note presents an inverse design methodology of metal nanostructures for localized surface plasmon resonances, based on the topology optimization approach. Using the proposed method, determination of the metal distribution in nanostructures is implemented for surface enhanced Raman spectroscopy to maximize the enhancement factor. The obtained results demonstrate that the outlined approach can be used to design metal nanostructure with resonant peak and significant enhancement factor at specified incident wavelength, and to control the shift of the resonant peak by topologically optimizing the nanostructure.

Keywords Topology optimization · Metal nanostructure · Localized surface plasmon resonances · Enhancement factor

1 Introduction

Localized surface plasmon resonances (LSPRs) are the strong interaction between metal nanostructures and visible light through the resonant excitations of collective oscillations of conduction electrons. In LSPRs, the local electromagnetic fields near the nanostructure can be many orders of magnitude higher than the incident fields, and the incident light around the resonant-peak wavelength is scattered strongly. The enhanced electric fields are confined within only a tiny region of the nanometer length scale near the surface of the nanostructures and decay significantly thereafter (Su et al. 2003). LSPRs of gold and silver nanoparticles were employed in stained-glass manufacture in the Middle Ages. Recently, the LSPR effect of metal nanostructures has been employed for many applications, including biomolecular manipulation and labeling (Cao et al. 2002), surface enhanced Raman spectroscopy (SERS) (Moskovits 1985), chemical and biological sensors (Elghanian et al. 1997), photovoltaics (Brongersma et al. 2000), near-field lithography and imaging (Ricard et al. 1985), optical trapping (Novotny et al. 1997; Miao and Lin 2007), nano optic circuits (Aizprua et al. 2003). LSPR and its enhancement of the electric field strongly depends on the size and shape of the metal nanostructure with fixed material properties and surrounding medium (Kottman et al. 2001; Mock et al. 2003; Mandal and Ramakrishna 2011). In the quest for enhancement of the electric field, a multitude of papers have reported parametric studies on various nanoparticle, nanoeipsoid, nanorod, nanotriangles and nanocrescent (Stockman 2004; Vogel and Gramotnev 2008; Lindquist et al. 2010; Lu et al. 2005). However, consideration of the inverse problem on finding the optimized spatial distribution of metal material in air or dielectric to cater to the performance

✉ Yongbo Deng
yongbo_deng@hotmail.com

¹ State Key Laboratory of Applied Optics, Changchun Institute of Optics, Fine Mechanics and Physics (CIOMP), Chinese Academy of Sciences, Changchun 130033, China

² Changchun Institute of Optics, Fine Mechanics and Physics (CIOMP), Chinese Academy of Sciences, Changchun 130033, China

³ Department of Mechanical and Industrial Engineering, Northeastern University, Boston, MA 02115, USA

⁴ Department of Electrical and Computer Engineering, Northeastern University, Boston, MA 02115, USA

⁵ Institute of Microstructure Technology, Karlsruhe Institute of Technology (KIT), Hermann-von-Helmholtzplatz 1, 76344, Eggenstein-Leopoldshafen, Germany

requirement (e.g. maximize the surface enhancement of electric field) is still deficient.

In this paper, the solid isotropic material with penalization like (SIMP-like) topology optimization approach is utilized to solve the inverse problem and determine the geometry of the nanostructure for LSPRs. SIMP-like topology optimization approach has been successfully applied in various fields of research, including elastics (Bendsøe 1989), hydrodynamics (Borrvall and Petersson 2003; Deng et al. 2011) and electromagnetics (Andkjær and Sigmund 2011). SIMP-like topology optimization approach finds the optimized structural topology with highly complex non-analytic partial differential equation described physical field by interpolating different materials with design variable (Bendsøe and Sigmund 2003). The design variable, usually varying continuously in $[0, 1]$ with 0 and 1 respectively represents two different materials, is evolved to an approximated indicator function using the gradient based optimization algorithm. The optimized solution can then be analyzed to foster the understanding of underlying physical principles.

2 Methodology

For electromagnetic waves propagating in the x-y plane, TM (H field in the z direction) polarized waves can excite the surface plasmon resonances of metal nanostructures. Periodicity of metal nanostructures plays a crucial role in tuning the optical response; and single metal nanostructure can be approximated by the periodic case with low volume ratio of the metal nanostructure. Therefore, the two dimensional periodic metal nanostructures are considered for LSPRs in this paper (Fig. 1). The scattered-field formulation is used in order to reduce the dispersion error

$$\nabla \cdot \epsilon_r^{-1} \nabla (H_z^s + H_z^i) + k_0^2 \mu_r (H_z^s + H_z^i) = 0, \text{ in } \Omega \quad (1)$$

where $H_z = H_z^s + H_z^i$ is the total field, H_z^s and H_z^i are the scattered and incident fields, respectively; ϵ_r and μ_r are the relative permittivity and permeability, respectively; $k_0 = \omega \sqrt{\epsilon_0 \mu_0}$ is the free space wave number with ω , ϵ_0 and μ_0 representing the angular frequency, free space permittivity and permeability, respectively; \mathbf{n} is the unit outward normal vector at $\partial\Omega$. The periodic boundary condition for the scattered-field is imposed on the two piecewise pairs of the computational boundary $\partial\Omega$. The incident field can be obtained by solving the Helmholtz equation in free space, and it is set to be the parallel-plane wave in this paper

$$H_z^i = H_0 e^{-jk_0 \mathbf{k} \cdot \mathbf{x}} \quad (2)$$

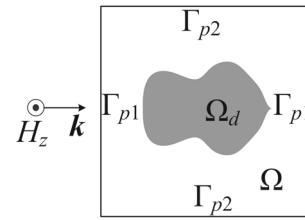


Fig. 1 Schematic for the computational domain of the periodic metal nanostructures for LSPRs, where Ω is the computational domain; $\Omega_d \subset \Omega$ is the design domain; \mathbf{k} is the wave vector; periodic boundary condition of the scattered-field is imposed on the boundary pairs Γ_{p1} and Γ_{p2} , respectively

where H_0 , set to be 1 in this paper, is the amplitude of the wave; $j = \sqrt{-1}$; $\mathbf{k} = (k_x, k_y)$ is the normalized directional wave vector; and $\mathbf{x} = (x, y)$ is the spatial position vector.

The SIMP-like topology optimization of metal nanostructures for LSPRs is implemented based on the material interpolation between the metal and free space or dielectric. In LSPRs, the used noble metal is usually nonmagnetic, e.g. Ag and Au. Therefore, the permeability is set to be 1. Then, only the spatial distribution of relative permittivity is varied iteratively in the evolution process of the design variable representing the topology of the metal nanostructure. In the visible light region, the relative permittivity of noble metal can be described by the Drude model

$$\epsilon_{rm}(\omega) = \epsilon_{r\infty} - \frac{\omega_p^2}{\omega(\omega - j\gamma_c)} \quad (3)$$

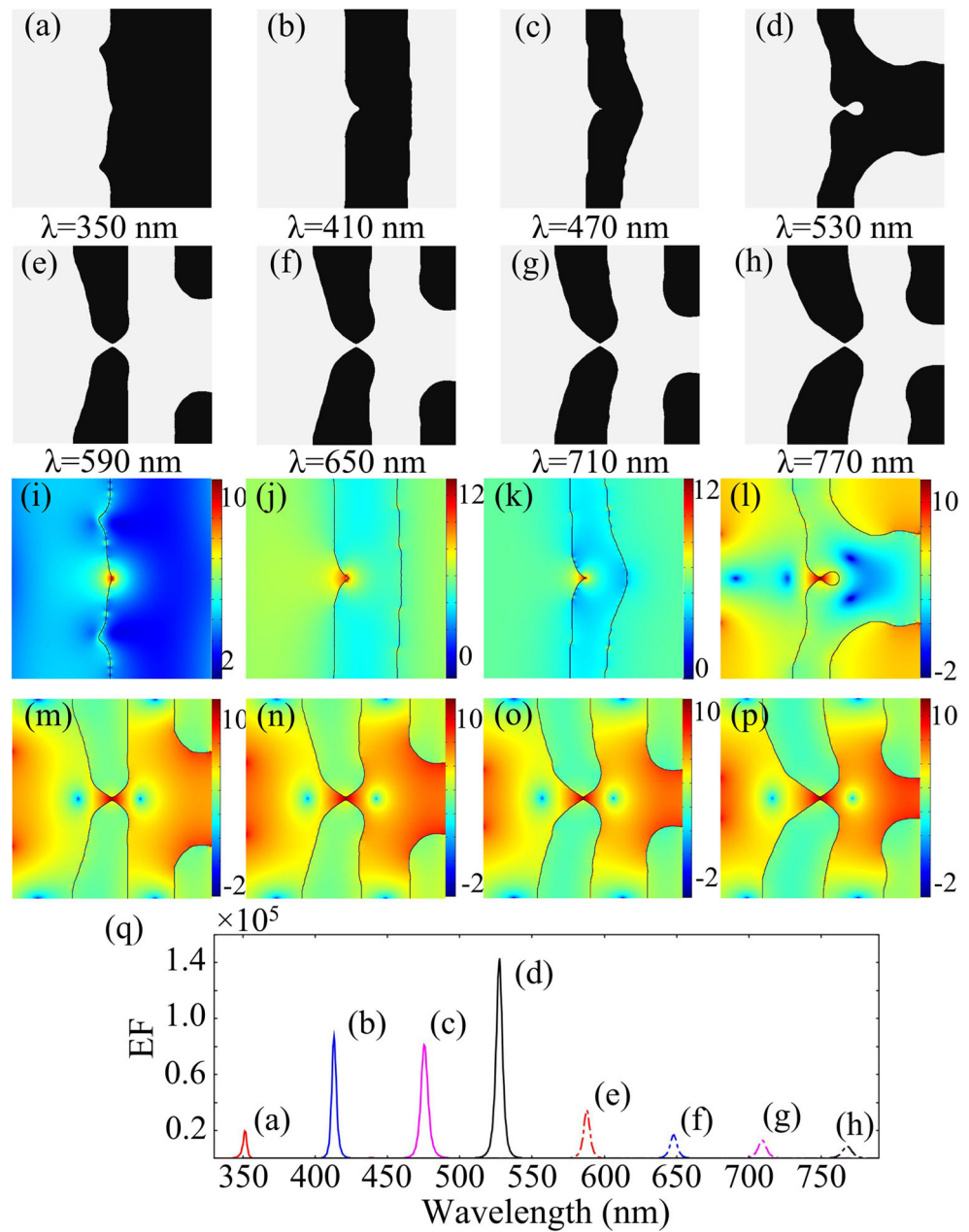
where ϵ_{rm} is the relative permittivity of metal; $\epsilon_{r\infty}$ is the high-frequency bulk permittivity; ω is the angular frequency of the incident wave; ω_p is the bulk plasmon frequency; γ_c is the collision frequency. The design variable ρ is introduced as a relative material density to interpolate between free space or dielectric permittivity ϵ_{rd} corresponding to $\rho = 0$ and metal permittivity ϵ_{rm} corresponding to $\rho = 1$. For surface plasmons, the electromagnetic field decays exponentially; hence, the material interpolation should decays rapidly away from $\rho = 1$ to mimic the metal surface. Thus, the material interpolation is implemented in the hybrid of logarithmic and power law approaches

$$\epsilon_r(\omega) = 10^{\log \epsilon_{rm}(\omega) - \frac{1-\rho^n}{1+\rho^n} [\log \epsilon_{rm}(\omega) - \log \epsilon_{rd}(\omega)]} \quad (4)$$

where n is the penalty and it is chosen to be 3 based on our numerical experiments. During the evolution of the design variable, the density filter and threshold projection are introduced to remove the gray area and enforce a minimum length scale of the obtained design (Lazarov and Sigmund 2011; Guest et al. 2004; Sigmund 2007).

SERS is one typical application of LSPRs (Moskovits 1985). In the following, the enhancement of SERS is carried out using the topology optimization approach for the nanostructures of LSPRs. In SERS, the strength of LSPRs

Fig. 2 (a)–(h) Optimized topologies of the SERS silver cells corresponding to different incident wavelengths in the visible light region, where the EF is maximized at the center of the design domain chosen to be the same as the square computational domain; (i)–(p) distribution of MOEF corresponding to the topologically optimized cells in (a)–(h), respectively; (q) EF spectra of the topologically optimized nanostructures at the specified enhancement position



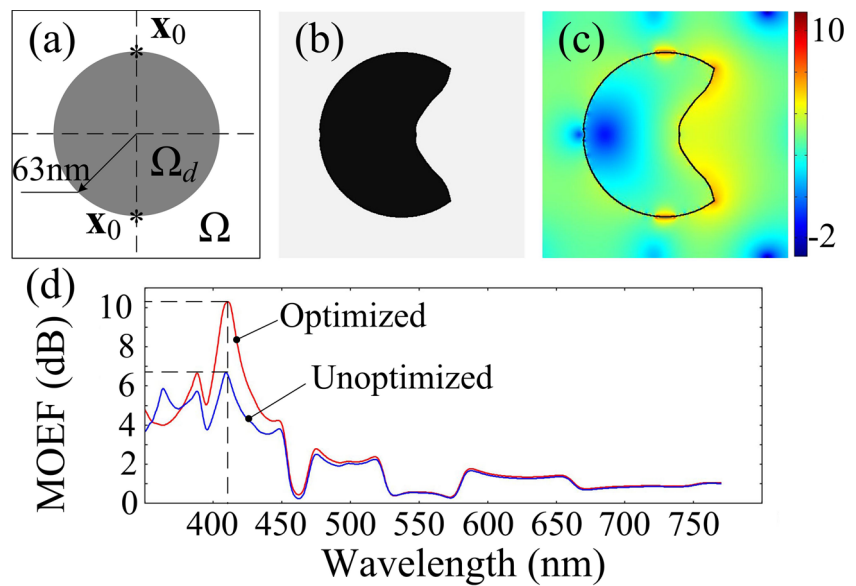
can be measured by the maximal enhancement factor (EF) defined as $\sup_{\mathbf{x} \in \Omega} \frac{|\mathbf{E}|^4}{E_0^4}$, where \mathbf{E} is the total electric field and $E_0 = \sqrt{\mu_0/\epsilon_0}$ is the amplitude of the incident electric wave. Then the topology optimization objective should be chosen to maximize $EF = \frac{|\mathbf{E}|^4}{E_0^4} \Big|_{\mathbf{x}=\mathbf{x}_0} = \int_{\Omega} \frac{|\mathbf{E}|^4}{E_0^4} \delta(\mathbf{x} - \mathbf{x}_0) d\Omega$, where \mathbf{x}_0 is the reasonably chosen enhancement position in Ω ; $\delta(\cdot)$ is the Dirac function; $dist(\mathbf{x}, \mathbf{x}_0)$ is the L_2 distance between the point $\forall \mathbf{x} \in \Omega$ and the specified position \mathbf{x}_0 . The enhancement position \mathbf{x}_0 should be chosen at the surface or coupling position of nanostructures, because the maximal EF must be at the metal surface or coupling position in LSPRs. In order to ensure the numerical stability

of the optimization procedure, the optimization objective is equivalently chosen to optimize the magnitude order of the normalized EF

$$\Phi = \log \left[\frac{1}{f_{e0}} \int_{\Omega} \frac{|\mathbf{E}|^4}{E_0^4} \delta(\mathbf{x} - \mathbf{x}_0) d\Omega \right] \tag{5}$$

where EF is normalized by f_{e0} ; and f_{e0} is the EF at \mathbf{x}_0 , corresponding to the nanostructure with metal material filled the design domain completely. Then the gradient-based optimization procedure, method of moving asymptotes (Svanberg 1987), is applied to update the design variable in an iterative approach, where the sensitivity is

Fig. 3 (a) Unoptimized nanodisk and the symmetrically chosen enhancement position \mathbf{x}_0 ; (b) topologically optimized nanodisk corresponding to the resonant-peak wavelength of the unoptimized nanodisk; (c) MOEF distribution of the optimized nanodisk, where the EF at the given enhancement position is 1.86×10^{10} and it is enhanced up to 3.89×10^3 times compared to that of the unoptimized nanodisk; (d) MOEF spectra of the optimized and unoptimized nanodisks in the visible light region



obtained using the continuous adjoint method. For details on the sensitivity analysis, one can refer to Deng et al. (2015).

3 Results and discussion

Using the topology optimization approach outlined, the cells of the periodic silver nanostructure for SERS are investigated in free space with relative permittivity equal to 1. The high-frequency bulk permittivity $\epsilon_{r\infty} = 6$, the bulk plasmon frequency $\omega_p = 1.5 \times 10^{16}$ rad/s, and the collision frequency $\gamma_c = 7.73 \times 10^{13}$ rad/s are obtained by fitting the experimental data in the literature (Johnson and Christy 1972; Liu et al. 2010). The side length of the square computational domain is set to be 190 nm. The computational domain is discretized using 200×200 quadrangular elements, where

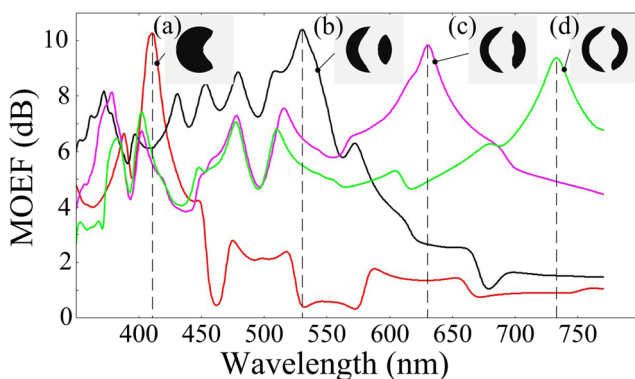
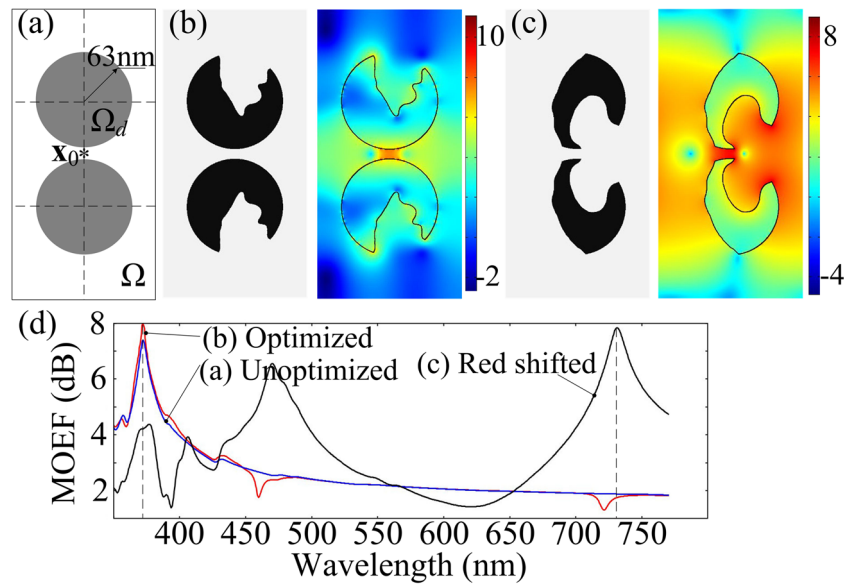


Fig. 4 MOEF spectra of the optimized nanodisks (a)–(d) respectively corresponding to the incident wavelengths equal to 410, 533, 633 and 733 nm, in which the resonant peak is red shifted by topologically optimizing the nanodisk at larger incident wavelength

the wave field variable is quadratically interpolated, and the design variable is linearly interpolated. The design domain is chosen to be the same as the computational domain (i.e. $\Omega_d = \Omega$). The incident TM wave is launched from the left boundary in the positive direction of the x -axis, and the maximal enhancement position is chosen to be the center of the square domain Ω . The incident wavelength is scanned in the visible light region (350 ~ 770 nm). For different incident wavelengths, the optimized topologies of the nanostructures are obtained as shown in Fig. 2a–h, with corresponding distribution of the magnitude order of EF (MOEF = \log EF) shown in Fig. 2i–p. For short incident wavelengths, the pit configuration is formed at the metal surface to increase the charge density and achieve LSPR at the enhancement position; the pit configuration is evolved to a tip-slit configuration as the increase of the incident wavelength, where two tips near the enhancement position are presented to increase the charge density, and a slit is formed between these two tips to enforce the given enhancement position to be the coupling position of the two tips and achieve LSPR based on the coupling effect. The EF spectra of the obtained optimized nanostructures shows that resonant peaks appear at the specified incident wavelengths (Fig. 2q). This illustrates the wavelength dependence of the optimized topology; and it can be concluded that the resonant peak can be achieved at a specified incident wavelength by the outlined topology optimization approach, and red or blue shift of the resonant peak can be controlled by specifying larger or smaller wavelength for the outlined topology optimization approach.

Currently, several nanostructures have been utilized to enhance LSPR, in which nanodisks are widely adopted in SERS to obtain high EF (Sarid and Challener 2010).

Fig. 5 (a) Unoptimized dual nanodisks and the enhancement position; (b) topologically optimized dual nanodisks and the corresponding MOEF distribution, at the resonant-peak wavelength of the unoptimized dual nanodisks; (c) topologically optimized dual nanodisks with incident wavelength equal to 733 nm and the corresponding MOEF distribution; (d) MOEF spectra of the unoptimized dual nanodisks and topologically optimized results in (b) and (c)



To demonstrate the superiority of the proposed inverse design approach for LSPRs, the nanodisk is topologically optimized for the silver material in the periodic cell. Figure 3b shows the topologically optimized nanodisk with incident wavelength set to be 410 nm, which is the resonant-peak wavelength of the unoptimized nanodisk shown in Fig. 3a. The distribution of MOEF and comparison of the MOEF spectra of the optimized and unoptimized nanodisks are respectively shown in Fig. 3c and d, where the EF is enhanced up to 3.89×10^3 times. The shift of the resonant peak can be realized by topologically optimizing the nanodisk at different incident wavelengths. Then three different additional incident wavelengths 533, 633 and 733 nm are respectively specified in the topology optimization of nanodisk. The nanodisk configuration and corresponding MOEF spectra are obtained as shown in Fig. 4, where the resonant peak is red shifted by evolving the topology and shape of the nanodisk with sequentially increased incident wavelength.

The coupling effect of dual nanostructures is one basic mechanism for the enhancement of LSPRs. Typical dual nanostructures include the dual nanodisks etc. (Sarid and Challener 2010). The topology optimization approach can be utilized to enhance the coupling effect of dual nanostructures, furthermore. Figure 5b shows the optimized topological configuration of the dual nanodisks and the corresponding distribution of MOEF, at the resonant-peak wavelength of the unoptimized dual nanodisks (Fig. 5a), where the coupling effect between nanodisks is strengthened by the topology optimization approach and EF is enhanced 3.73 times. The resonant peak achieved by the coupling effect of the dual nanostructures can also be shifted by specifying different incident wavelengths. The incident wavelength

733 nm is utilized and the topologically optimized dual nanodisks along with the corresponding MOEF distribution are obtained as shown in Fig. 5c. From the MOEF spectra shown in Fig. 5d, one can confirm that the resonant peak is red shifted by topologically optimizing of the dual nanodisks with larger incident wavelength.

4 Conclusion

In conclusion, the inverse design method based on topology optimization approach has been outlined for the determination of the metal material distribution in the nanostructure for LSPRs. Based on the proposed method, the topologically optimized nanostructure can be obtained with resonant peak at the specified incident wavelength. Red or blue shift of the resonant peak can be controlled by specifying larger or smaller wavelength for the outlined topology optimization approach. Therefore, the outlined approach can be used to design nanostructure with resonant peak and enhanced enhancement factor at specified incident wavelength and control the shift of the resonant peak by topologically optimizing the nanostructure. This inverse design method of nanostructures for LSPRs can be further extended to other plasmonic nanostructures, e.g. optical antenna and optical trapping.

Acknowledgments This work is supported by the Open Fund of SKLAO, the National Natural Science Foundation of China (No. 51405465, 51275504), Science and Technology Development Plane of JiLin Province (No. 20140519007JH) and the National High Technology Program of China (No. 2015AA042604).

References

- Aizpruua J, Hanarp P, Sutherland DS, Kall M, Bryant GW, Garcia de Agajo FJ (2003) Optical properties of gold nanorings. *Phys Rev Lett* 90:057401
- Andkjær J, Sigmund O (2011) Topology optimized low-contrast all-dielectric optical cloak. *Appl Phys Lett* 98:021112
- Bendsøe M (1989) Optimal shape design as a material distribution problem. *Struct Optim* 1:193–202
- Bendsøe M, Sigmund O (2003) *Topology optimization-theory methods and applications*. Springer, Berlin
- Borrvall T, Petersson J (2003) Topology optimization of fluids in Stokes flow. *Int J Numer Methods Fluids* 41:77–107
- Brongersma ML, Hartman JW, Atwater HA (2000) Electromagnetic energy transfer and switching in nanoparticle chain arrays below the diffraction limit. *Phys Rev B* 62:R16356
- Cao YWC, Jin RC, Mirkin CA (2002) Nanoparticles with Raman spectroscopic fingerprints for DNA and RNA detection. *Science* 297:1536
- Deng Y, Liu Z, Zhang P, Liu Y, Wu Y (2011) Topology optimization of unsteady incompressible Navier-Stokes flows. *J Comput Phys* 230:6688–6708
- Deng Y, Liu Z, Song C, Wu J, Liu Y, Wu Y (2015) Topology optimization-based computational design methodology for surface plasmon polaritons. *Plasmonics* 10:569–583
- Elghanian R, Storhoff JJ, Mucic RC, Letsinger RL, Mirkin CA (1997) Selective colorimetric detection of polynucleotides based on the distance-dependent optical properties of gold nanoparticles. *Science* 227:1078
- Guest J, Prevost J, Belytschko T (2004) Achieving minimum length scale in topology optimization using nodal design variables and projection functions. *Int J Numer Methods Eng* 61:238–254
- Johnson PB, Christy RW (1972) Optical constants of the noble metals. *Phys Rev B* 6:4370–4379
- Kottman JD, Martin OJF, Smith DR, Schultz S (2001) Dramatic localized electromagnetic enhancement in plasmon resonant nanowires. *Chem Phys Lett* 341:1
- Lazarov B, Sigmund O (2011) Filters in topology optimization as a solution to Helmholtz type differential equations. *Int J Numer Methods Eng* 86:765–781
- Lindquist NC, Nagpal P, Lesuffleur A, Norris DJ, Oh SH (2010) Three-dimensional plasmonic nanofocusing. *Nano Lett* 10:1369–1373
- Liu Y, Zentgraf T, Bartal G, Zhang X (2010) Transformational plasmon optics. *Nano Lett* 10:1991–1997
- Lu Y, Liu GL, Kim J, Mejia YX, Lee LP (2005) Nanophotonic crescent moon structures with sharp edge for ultrasensitive biomolecular detection by local electromagnetic field enhancement effect. *Nano Lett* 5:119
- Mandal P, Ramakrishna SA (2011) Dependence of surface enhanced Raman scattering on the plasmonic template periodicity. *Opt Lett* 36:3705–3707
- Miao X, Lin LY (2007) Large dielectrophoresis force and torque induced by localized surface plasmon resonance of Au nanoparticle array. *Opt Lett* 32:295–297
- Mock JJ, Smith DR, Schultz S (2003) Local refractive index dependence of plasmon resonance spectra from individual nanoparticles. *Nano Lett* 3:485
- Moskovits M (1985) Surface-enhanced spectroscopy. *Rev Mod Phys* 57:783
- Novotny L, Bain RX, Xie XS (1997) Theory of nanometric optical tweezers. *Phys Rev Lett* 79:645
- Ricard D, Roussignol P, Flytzanis C (1985) Surface-mediated enhancement of optical phase conjugation in metal colloids. *Opt Lett* 10:511
- Sarid D, Challener W (2010) *Modern introduction to surface plasmons: theory, Mathematica modelling and applications*. Cambridge University Press
- Sigmund O (2007) Morphology-based black and white filters for topology optimization. *Struct Multidisc Optim* 33:401–424
- Stockman MI (2004) Nanofocusing of optical energy in tapered plasmonic waveguides. *Phys Rev Lett* 93:137404
- Su KH, Wei QH, Zhang X, Mock JJ, Smith DR, Schultz S (2003) Interparticle coupling effects on plasmon resonances of nanogold particles. *Nano Lett* 3:1087–1090
- Svanberg K (1987) The method of moving asymptotes—a new method for structural optimization. *Int J Numer Methods Eng* 24:359–373
- Vogel MW, Gramotnev DK (2008) Optimization of plasmon nanofocusing in tapered metal rods. *J Nanophotonics* 2:021852